




## The Drosophila histone variant H2A.V works in concert with HP1 to promote kinetochore-driven microtubule formation

Fiammetta Verni & Giovanni Cenci


To cite this article: Fiammetta Verni & Giovanni Cenci (2015) The Drosophila histone variant H2A.V works in concert with HP1 to promote kinetochore-driven microtubule formation, Cell Cycle, 14:4, 577-588, DOI: [10.4161/15384101.2014.991176](https://doi.org/10.4161/15384101.2014.991176)

To link to this article: <http://dx.doi.org/10.4161/15384101.2014.991176>

 View supplementary material [↗](#)

 Accepted author version posted online: 15 Jan 2015.

 Submit your article to this journal [↗](#)

 Article views: 179

 View related articles [↗](#)

 View Crossmark data [↗](#)

# The *Drosophila* histone variant H2A.V works in concert with HP1 to promote kinetochore-driven microtubule formation

Fiammetta Verni<sup>1,\*</sup> and Giovanni Cenci<sup>1,2</sup>

<sup>1</sup>Dipartimento di Biologia e Biotecnologie “C. Darwin”; Sapienza Università di Roma; Roma, Italy; <sup>2</sup>Sbarro Institute for Cancer Research and Molecular Medicine; Department of Biology; Temple University; Philadelphia, PA USA

**Keywords:** chromosome segregation, *Drosophila*, H2A.V, HP1, mitosis

Unlike other organisms that have evolved distinct H2A variants for different functions, *Drosophila melanogaster* has just one variant which is capable of filling many roles. This protein, H2A.V, combines the features of the conserved variants H2A.Z and H2A.X in transcriptional control/heterochromatin assembly and DNA damage response, respectively. Here we show that mutations in the gene encoding H2A.V affect chromatin compaction and perturb chromosome segregation in *Drosophila* mitotic cells. A microtubule (MT) regrowth assay after cold exposure revealed that loss of H2A.V impairs the formation of kinetochore-driven (k) fibers, which can account for defects in chromosome segregation. All defects are rescued by a transgene encoding H2A.V that lacks the H2A.X function in the DNA damage response, suggesting that the H2A.Z (but not H2A.X) functionality of H2A.V is required for chromosome segregation. We also found that loss of H2A.V weakens HP1 localization, specifically at the pericentric heterochromatin of metaphase chromosomes. Interestingly, loss of HP1 yielded not only telomeric fusions but also mitotic defects similar to those seen in H2A.V null mutants, suggesting a role for HP1 in chromosome segregation. We also show that H2A.V precipitates HP1 from larval brain extracts indicating that both proteins are part of the same complex. Moreover, we found that the overexpression of HP1 rescues chromosome missegregation and defects in the kinetochore-driven k-fiber regrowth of H2A.V mutants indicating that both phenotypes are influenced by unbalanced levels of HP1. Collectively, our results suggest that H2A.V and HP1 work in concert to ensure kinetochore-driven MT growth.

## Introduction

Eukaryotic chromatin contains basic units called nucleosomes, consisting of octamers of 4 core histones with 146 base pair stretches of DNA wrapped around them.<sup>1,2</sup> The chromatin's function and structure are determined by histone modifications such as acetylation, methylation, phosphorylation, and ubiquitylation,<sup>3,4</sup> and the subsequent binding of specific factors to modified histones promotes further changes in chromatin organization.<sup>5</sup> In addition to histone post-translational modifications, histone variants have recently emerged as important determinants of chromatin composition.<sup>6</sup> Variants of H3 and H2A histones are to date the best characterized. Among them, H2A.Z, the highly evolutionarily conserved variant of the canonical histone H2A,<sup>7</sup> is unique in representing the only variant required for viability and development in several organisms.<sup>8–11</sup> Mounting evidence has demonstrated that H2A.Z is implicated in multiple cellular pathways such as maintenance of chromosome stability and segregation,<sup>12–14</sup> modulation of transcription (for a review see Refs<sup>15,16</sup>), as well as regulation of heterochromatin

spreading.<sup>17–19</sup> However, though H2A.Z plays a role in different pathways, its functional mechanisms have not been fully elucidated.

*Drosophila melanogaster* has a single H2A.Z variant, H2A.V that represents 5–10% of cellular H2A proteins. In addition to sharing structural similarities with metazoan H2A.Z, H2A.V also harbors a 4 amino acid stretch at the end of its extended tail domain that resembles the canonical phosphorylation motif found in the H2A.X variant histones (for a recent review see Ref<sup>20</sup>). This site contains a serine residue (S137), which is phosphorylated by ATM and ATR kinases following DNA break and repair, indicating that H2A.V, like its counterpart H2A.X, acts as a DNA damage sensor.<sup>21,22</sup> Similar to mammalian H2A.Z, H2A.V nonrandomly localizes to heterochromatin regions and many euchromatin regions on polytene chromosomes.<sup>23</sup> Genome-wide chromatin immunoprecipitation studies revealed that H2A.V is associated with constitutively expressed genes as well as developmental silenced loci. H2A.V levels appeared reduced at the promoters of induced heat shock genes indicating that, like its human H2A.Z ortholog, this variant is depleted from chromatin upon activation of transcription.<sup>24,25</sup> Finally, it

\*Correspondence to: Fiammetta Verni; Email: fiammetta.verni@uniroma1.it; Giovanni Cenci; Email: giovanni.cenci@uniroma1.it

Submitted: 08/20/2014; Revised: 11/16/2014; Accepted: 11/20/2014

<http://dx.doi.org/10.4161/15384101.2014.991176>

has been reported that *H2A.V* behaves genetically as a *PcG* gene and that mutations in *H2A.V* suppress position effect variegation. In addition *H2A.V* mutants exhibit reduced H3 lysine 9 (H3K9) methylation and reduced binding of HP1 and Pc suggesting that this H2A histone variant is required for euchromatic silencing and heterochromatin formation.<sup>26</sup> Thus, it appears that *Drosophila* *H2A.V* fulfills several distinct functions and combines the features of *H2A.Z* in transcriptional control with the functions of *H2A.X* in DNA damage response.<sup>20</sup>

Here we demonstrate that loss of *H2A.V* causes missegregation defects in *Drosophila* neuroblast cells highlighting an unanticipated function of *H2A.Z*, but not of *H2A.X*, in *Drosophila* cell division. We found that *H2A.V* mutant chromosomes fail to align at the metaphase plate and show reduced HP1 localization as well as a delayed kinetochore-driven microtubule re-growth after cold treatment. Consistently, we provide evidence that *HP1* mutant neuroblasts demonstrate defects in kinetochore-driven MT growth, similar to the effect observed in *H2A.V* mutants. We furthermore show that *H2A.V* forms a complex with HP1 and that overexpression of HP1 substantially reduces the cell division defects of *H2A.V* mutants. These results suggest that *H2A.V* stabilizes HP1 binding to chromatin. Thus, our findings indicate that in *Drosophila* *H2A.V* and HP1 cooperate to regulate chromosome segregation and reveal a new role for HP1 in the assembly of mitotic spindle.

## Results

### Loss of *H2A.V* affects chromosome segregation in *Drosophila* mitotic cells

To investigate whether *H2A.V* regulates heterochromatin organization in mitotic chromosomes, we conducted a cytological analysis of metaphase spreads from the *H2A.V*<sup>810</sup> null mutant.<sup>23,26</sup> Colchicine-treated *H2A.V*<sup>810</sup> homozygous and *H2A.V*<sup>810</sup>/*Dff(3R)TI-P* hemizygous larval brains exhibited a plethora of mitotic abnormalities, which are depicted in **Figure 1A**. In a significant portion of mutant mitotic cells (~10%; n = 850), centromeric chromatin appeared poorly condensed giving rise to evident DAPI staining discontinuities which have the appearance of chromatin gaps (**Fig. 1Ab, B**). In addition, ~30% of mutant cells exhibited irregular condensation of both euchromatic and heterochromatic regions of chromosomes. We also observed cells with overcondensed chromosomes (~7%), precocious sister chromatid separation and rare chromosome breaks (**Fig. 1Ac,d, B**). Taken together with recent studies showing that *H2A.V* may participate in chromatin remodeling,<sup>27</sup> these results indicate that *H2A.V* plays a global role in the organization of chromatin. To assess whether loss of *H2A.V* affected cell cycle progression, we measured the Mitotic Index (MI) and the Anaphases Frequency (AF) in no-colchicine treated DAPI-stained *H2A.V*<sup>810</sup> homozygous and *H2A.V*<sup>810</sup>/*Dff(3R)TI-P* hemizygous larval brains. During this characterization, we found that *H2A.V*<sup>810</sup> mutant brains, in addition to distinct prometaphase, metaphase and anaphase cells, contained unique cells (14%, n = 900) with chromosomes and/or chromatids scattered along the

major axis of the cell. This result suggests that either chromosome congression or segregation, or both, are influenced during mitosis (**Fig. 1B,C; Supplementary Fig. 1A**). Yet, as we could not unambiguously define these figures as anaphases (see also below), we included them only in the total number of dividing cells. When we calculated the mitotic parameters we found that in the *H2A.V*<sup>810</sup> mutant brains the MI was indistinguishable from wild type, whereas the frequency of anaphases showed a mild, but statistically significant (~20%), reduction compared to wild-type cells (n = 900; **Fig. 1C**). Thus, although *H2A.V* depleted cells can normally enter mitosis, a small percentage of mutant cells either fail to complete mitosis or exhibit a delayed anaphase onset. All *H2A.V*<sup>810</sup> mutant mitotic abnormalities were rescued by a wild-type *H2A.V-GFP* transgene<sup>9</sup> indicating that they were indeed caused by an *H2A.V* depletion. Interestingly, the *H2A.V*<sup>810</sup> mutant phenotypes were also rescued by a transgene that encodes *H2A.V* with a C-terminal truncation and therefore lacking of *H2A.X* function<sup>9</sup> (**Fig. 1B, C and E**). This suggests that it is the loss of *H2A.Z* function, not *H2A.X*, that affects chromosome behavior.

### *H2A.V* mutants exhibit defects in the organization of kinetochore-driven MTs

To assess whether chromosome segregation defects were due to defective spindles, we immunostained *H2A.V*<sup>810</sup> mutant neuroblasts with anti- $\alpha$  tubulin and anti-Spd2 antibodies, which recognize spindle fibers and centrosomes, respectively.<sup>28</sup> This analysis confirmed the presence of cells (~15%; n = 300, **Fig. 1C–E**) with chromosomes scattered across the mitotic spindles. We have also found that a small percentage of dividing *H2A.V*<sup>810</sup> mutant cells displayed monopolar spindles (~5%; n = 300; **Fig. 1Dd, E**) indicating that the absence of *H2A.V* leads to a mild spindle disorganization. However, nearly every cell with dispersed chromosomes contained normal bipolar spindles (**Fig. 1D, E**), suggesting that chromosome misalignment in *H2A.V*<sup>810</sup> mutants is not due to spindle defects. To test whether this defective chromosome behavior was due to a reduction of MTs, we measured the density of MTs in wild-type and mutant metaphases and found that it did not generally vary between *H2A.V*<sup>810</sup> mutant and wild-type cells. However the *H2A.V*<sup>810</sup> mutant cells with dispersed chromosomes represented an exception, as they exhibited a reduction of MT density (**Fig. 1Dc; Fig. S1B**), though this reduction was mild. To check whether the decreased MT density was related to a specific sub-set of MTs, we compared the spindle MT density with that of centrosomal MTs and found that MT density in mutant cells decreased mainly within the spindle (**Fig. S1B**). This last result suggests that a reduced number of kinetochore MTs could account for the chromosome misalignment seen in these mutant cells.

To better understand the mitotic phase of cells with misaligned chromosomes, we immunostained *H2A.V*<sup>810</sup> mutant cells for the spindle assembly checkpoint (SAC) proteins BubR1 and Zw10. This analysis revealed that all cells with misaligned chromosomes from homozygous or hemizygous *H2A.V*<sup>810</sup> mutant brains retain a robust centromeric localization of both BubR1 and Zw10 (**Fig. 2**). This indicates that in these cells the

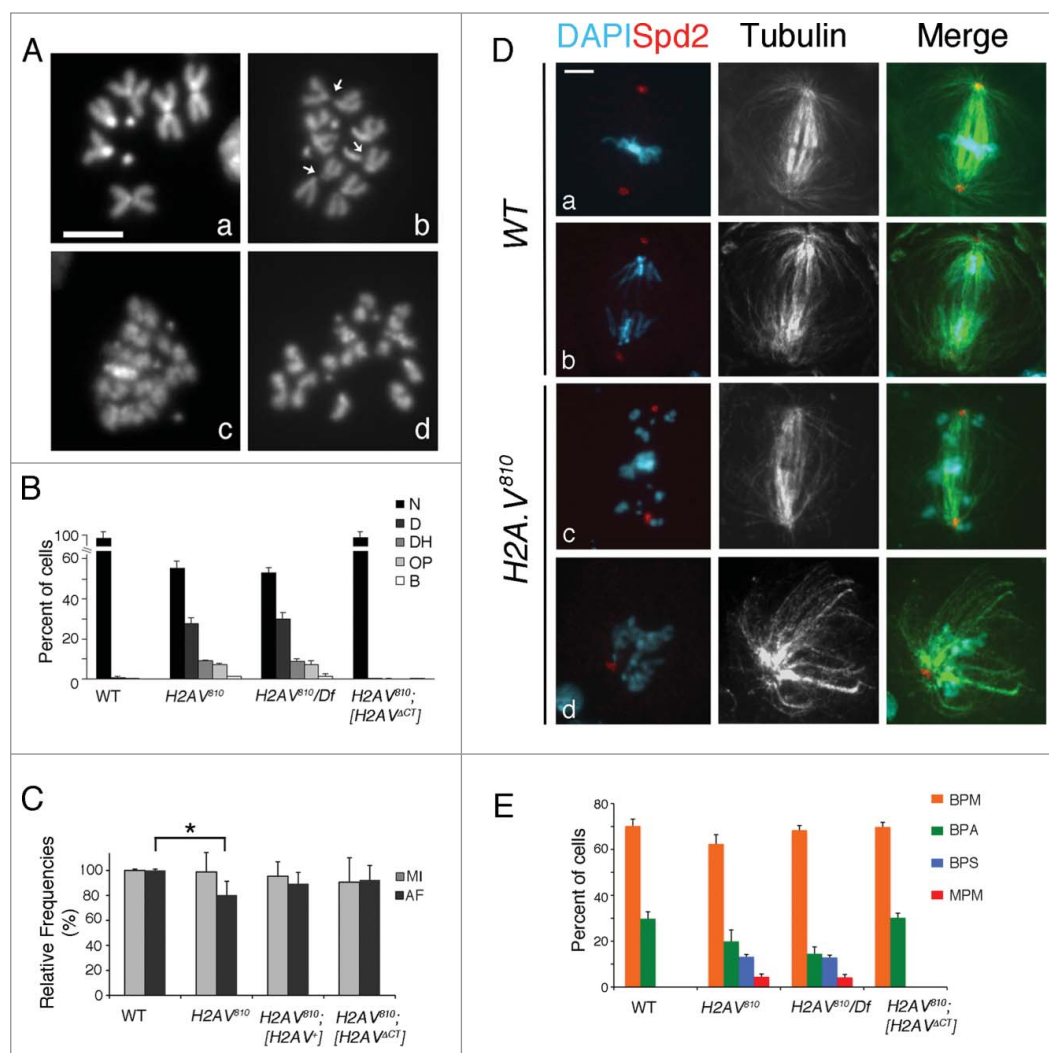


**Figure 1.** H2A.V is required for proper chromosome condensation and segregation. (A) DAPI stained colchicine-treated (Aa–d) mitotic cells from control (Aa), *H2A.V<sup>810</sup>* (Ab) and *H2A.V<sup>810</sup>/Df(3R)Tl-P* (Ac–d) mutant brains. *H2A.V* mutant metaphases exhibit chromosomes with poorly condensed centromeric chromatin (arrows in Ab), overcondensed chromosomes (Ac), or chromosomes with precocious sister chromatid separation (Ad). (B) Quantification of mitotic defects in *H2A.V* mutants and in *H2A.V* mutants also bearing a *H2A.V* transgene with a C-terminal truncation. See text for further details. N = Normal cells; D = Cells with poorly condensed chromosomes; DH = cells with chromosomes exhibiting decondensation at the pericentric region; OP = Cells showing either overcondensed chromosomes or precocious sister chromatid separation; B = Cells with chromosome breaks. (C) Mitotic Index (MI) and Frequency of Anaphases (AF) in WT, *H2A.V<sup>810</sup>*, *H2A.V<sup>810</sup> [H2A.V<sup>+</sup>]* and *H2A.V<sup>810</sup> [H2A.V<sup>ΔCT</sup>]* larval brain cells (\**P* < 0.01, t Student's Test). (D) Mitotic spindles of wild type (Da,b) and *H2A.V* mutant (Dc,d) stained for tubulin (green), Spd2 (red) and DAPI. (Da) Wild type metaphase; (Db) wild type anaphase; (Dc) a *H2A.V* mutant cell with scattered chromosomes; (Dd) a rare example of *H2A.V* mutant cell with a monopolar spindle. Bar = 5 μm. E) Quantification of spindle defects in WT, *H2A.V<sup>810</sup>* and *H2A.V<sup>810</sup> [H2A.V<sup>ΔCT</sup>]*. BPM = prometaphases/metaphases with normal bipolar spindles; BPA = ana/telophases with normal bipolar spindles; BPS = cells with dispersed chromosomes and normal bipolar spindles; MPM = metaphases and ana/telophases with monopolar spindles.

SAC is not satisfied thus preventing anaphase onset. Consistently, *H2A.V<sup>810</sup>* mutant neuroblasts with misaligned chromosomes exhibit high levels of cyclin B (Fig. S2), which is normally degraded at the metaphase-to-anaphase transition. Altogether, these data confirm that *H2A.V<sup>810</sup>* abnormal figures are in a pro/metaphase (rather than ana/telophase)-like stage, although most of them exhibit spindle length similar to that of anaphases.

tubule re-growth assay following cold-induced MT depolymerization in mitotic neuroblasts<sup>34</sup> and analyzed the MT growth from kinetochores. Consistent with published data,<sup>29,34</sup> we found that the formation of kinetochore-associated MT bundles precedes MT re-growth from the centrosomes. In particular, after 50 min of cold treatment MTs were completely depolymerized in a large proportion of both wild type and mutant brain cells

Nonetheless, for the sake of clarity, we will refer to them as pseudo-anaphases (PAs), a term used in previous studies characterizing similar effects.<sup>29,30</sup> We have also observed that in most mutant cells *Zw10* (40–80%; *n* = 40), although strongly associated with kinetochores, failed to migrate toward the spindle poles along the microtubules, as it normally does in control metaphases<sup>31,32</sup> (Fig. 2B, C). As it is known that *Zw10* streaming is due to the association of the SAC component to k-MTs, we hypothesized that loss of *Zw10* streaming reflected an improper organization of kinetochore fibers (k-fibers).

To confirm these results, we immunostained *H2A.V<sup>810</sup>* mutant cells with the augmin component *Dgt6*, a well-established marker for k-fibers in *Drosophila* cells.<sup>29,33</sup> Consistent with a recent work,<sup>29</sup> we found that in control cells *Dgt6* associates mainly with k-fibers (Fig. 3A). Interestingly, *H2A.V<sup>810</sup>* mutant cells exhibited a dramatic reduction of *Dgt6* localization during both metaphase and anaphase (Fig. 3A, B) indicating that the reduction of *Dgt6* in the mutant neuroblasts is likely due to defects in the k-fiber organization.

To verify whether k-fiber organization was impaired in *H2A.V<sup>810</sup>* mutants, we employed a spindle microtubule re-growth assay following cold-induced MT depolymerization in mitotic neuroblasts<sup>34</sup> and analyzed the MT growth from kinetochores. Consistent with published data,<sup>29,34</sup> we found that the formation of kinetochore-associated MT bundles precedes MT re-growth from the centrosomes. In particular, after 50 min of cold treatment MTs were completely depolymerized in a large proportion of both wild type and mutant brain cells

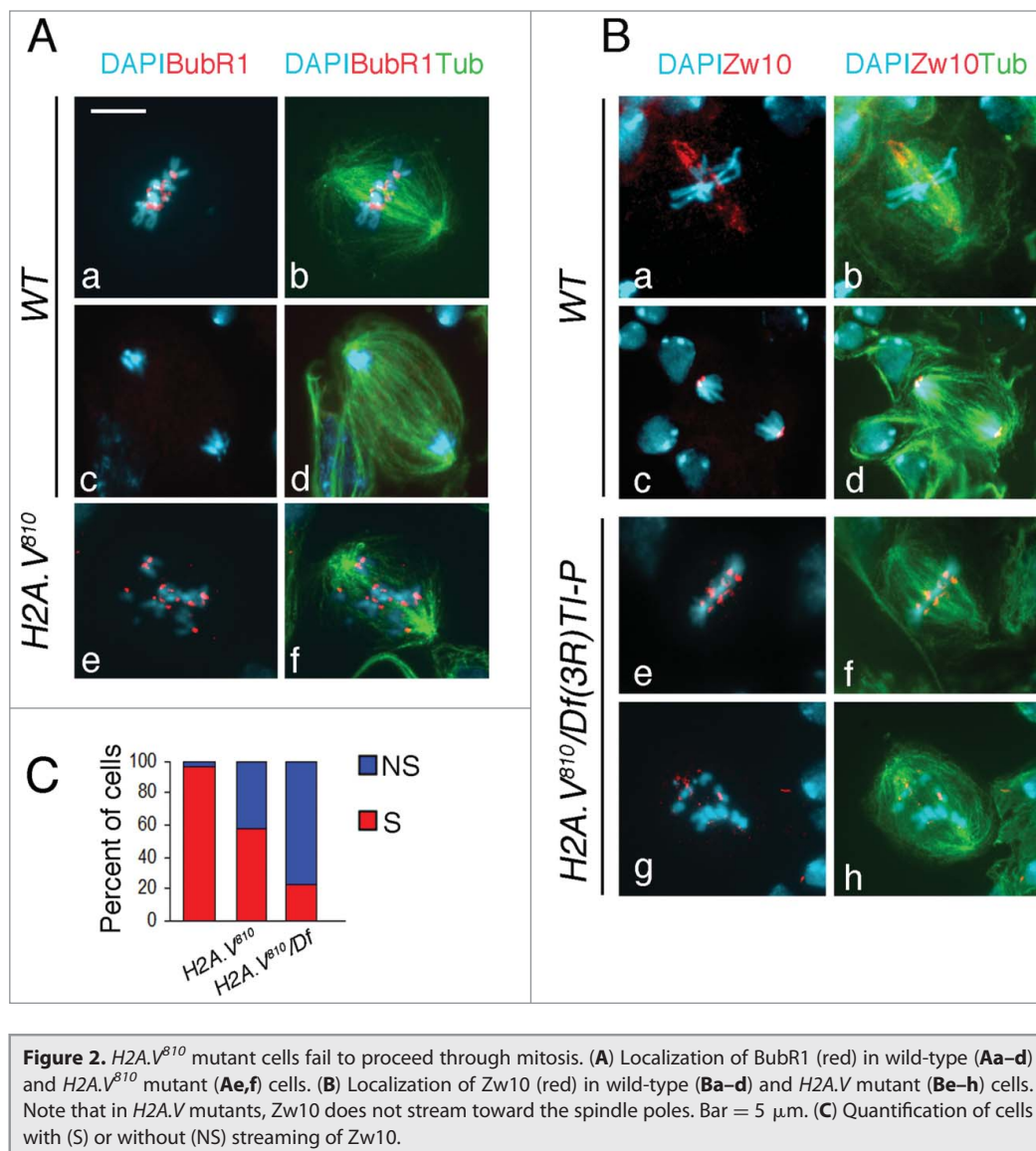


**Figure 2.** *H2A.V<sup>810</sup>* mutant cells fail to proceed through mitosis. (A) Localization of BubR1 (red) in wild-type (Aa–d) and *H2A.V<sup>810</sup>* mutant (Ae, f) cells. (B) Localization of Zw10 (red) in wild-type (Ba–d) and *H2A.V* mutant (Be–h) cells. Note that in *H2A.V* mutants, Zw10 does not stream toward the spindle poles. Bar = 5  $\mu$ m. (C) Quantification of cells with (S) or without (NS) streaming of Zw10.

that displayed only an array of short MTs associated to centrosomes (0 min; Fig. 4A, C). After returning to room temperature, differences between wild type and mutant cells emerged. In wild-type cells 1 min after returning to room temperature, we observed ~30% of cells ( $n = 250$ ) with MTs associated to centromeric regions, ~55% with MTs associated to both chromosomes and centrosomes and ~10% only to centrosomes. After 2 min we found the majority of cells (65%) elicited MTs associated with both chromosomes and centrosomes. Finally, after 5 min almost all wild type cells displayed a completely organized mitotic spindle, which appeared indistinguishable from that of untreated cells (Fig. 4A, C).

In 60% of *H2A.V<sup>810</sup>* mutant cells ( $n = 70$ ) that were recovered for 1 min at room temperature, MTs re-grew only from centrosomes whereas only a small percentage (6%) of mutant neuroblasts displayed MTs associated to chromosomes (Fig. 4B, C). This MT re-growth pattern was observed in cells with normal and irregular (PA) chromosome congression. After 2 min, the

number of cells with MT re-growth from centrosomes halved (from 60% to 30%), whereas the percentage of cells displaying MTs associated to chromosomes increased. Interestingly, few cells (~7%) with only kinetochore-associated MTs were found also after 5 and 10 min suggesting that *H2A.V<sup>810</sup>* mutant neuroblasts experienced a delay in the kinetochore-driven MT formation (Fig. 4B, C). As consequence, all mutant cells displayed fully developed spindles only after 30 min while in wild-type completely formed spindles were observed after 5 min (Fig. 4C).

#### H2A.V forms a complex with HP1

Given the defects in the organization of k-fibers observed upon loss of *H2A.V*, we hypothesized that this effect was precipitated by an improper recruitment of *Drosophila* centromere/kinetochore proteins. To test this, we verified the localization of representative centromere factors (Cid/Cenp-A, Cenp-C), and inner (Mis12, Nls1), or outer (Ndc80/Hec1) plate components. Immunofluorescence experiments showed that all tested centromere/kinetochore proteins localize normally in *H2A.V<sup>810</sup>* mutant PA chromosomes (Fig. S3), as well as in normally condensed mutant chromosomes, indicating that chromosome missegregation is not a consequence of loss of these centromere/kinetochore proteins.

Previous studies demonstrated that depletion of *H2A.Z* in mammalian cells disrupts Heterochromatin Protein 1 $\alpha$  (HP1 $\alpha$ )-chromatin interactions at chromosomal arms and pericentric regions.<sup>13</sup> In addition *Drosophila* *H2A.V* was shown to be important for recruiting HP1 (the *Drosophila* ortholog of mammalian HP1 $\alpha$ ) on polytene chromosome chromocenter.<sup>26</sup> Thus, we wanted to investigate whether an *H2A.V*-HP1 functional relationship could account for the cytological phenotypes observed in *H2A.V<sup>810</sup>* mutant cells.

By immunostaining wild-type larval brain cells with the mouse monoclonal anti-HP1 antibody C1A9, we found that HP1 is strongly enriched at heterochromatin regions (chromocenter) of

interphase nuclei. HP1 strongly localizes also to pericentric regions of mitotic chromosomes from prometaphase to anaphase (Fig. 5A-C). In particular, we found that HP1 staining at heterochromatin regions peaks during anaphase, likely as a consequence of a physiological centromere clustering (Fig. 5H). In addition, HP1 staining is also found along all chromosome arms, including chromosome ends, although this localization pattern is not as intense as at heterochromatin regions. HP1 immunostaining in *H2A.V* mutant brain cells revealed a severe reduction of HP1 localization at both heterochromatic and euchromatic regions of *H2A.V*<sup>B10</sup> homozygous (75% of cells; n = 250) and hemizygous (70% of cells; n = 150) mitotic chromosomes with respect to wild type (15% of cells; n = 200; Fig. 5D-G). In particular, the intensity of HP1 staining decreased mainly during metaphase and anaphase (Fig. 5H), but not in prophase and interphase. This indicates that the reduction of HP1 localization at centromeres upon loss of *H2A.V* occurs preferentially during mitosis.

Based on our anti-HP1 immunofluorescence analyses, we then asked whether *H2A.V* and HP1 could interact. GFP-trap mediated immunoprecipitation of *H2A.V* from *H2A.V*-GFP expressing brain extracts revealed that *H2A.V* is able to precipitate HP1, suggesting that both proteins are part of the same complex (Fig. 6A). The HP1 protein consists of an N-terminal Chromo Domain (CD) separated from a related C-terminal Chromo Shadow Domain (CSD) by a hinge region (H). All three domains are required for specific and different HP1 functions and interactions<sup>35</sup> (Fig. 6B). Interestingly, pulldown experiments using a GST-tagged HP1 (GST-HP1) and HP1 truncations (namely, GST-HP1<sup>ΔCD</sup>, -HP1<sup>ΔH</sup> and -HP1<sup>ΔCSD</sup>, which lack of the N-terminal CD, hinge or C-terminal CSD domains, respectively) revealed that *H2A.V* is not precipitated by HP1 when it lacks the CD domain, indicating that the HP1-*H2A.V* interaction is mediated

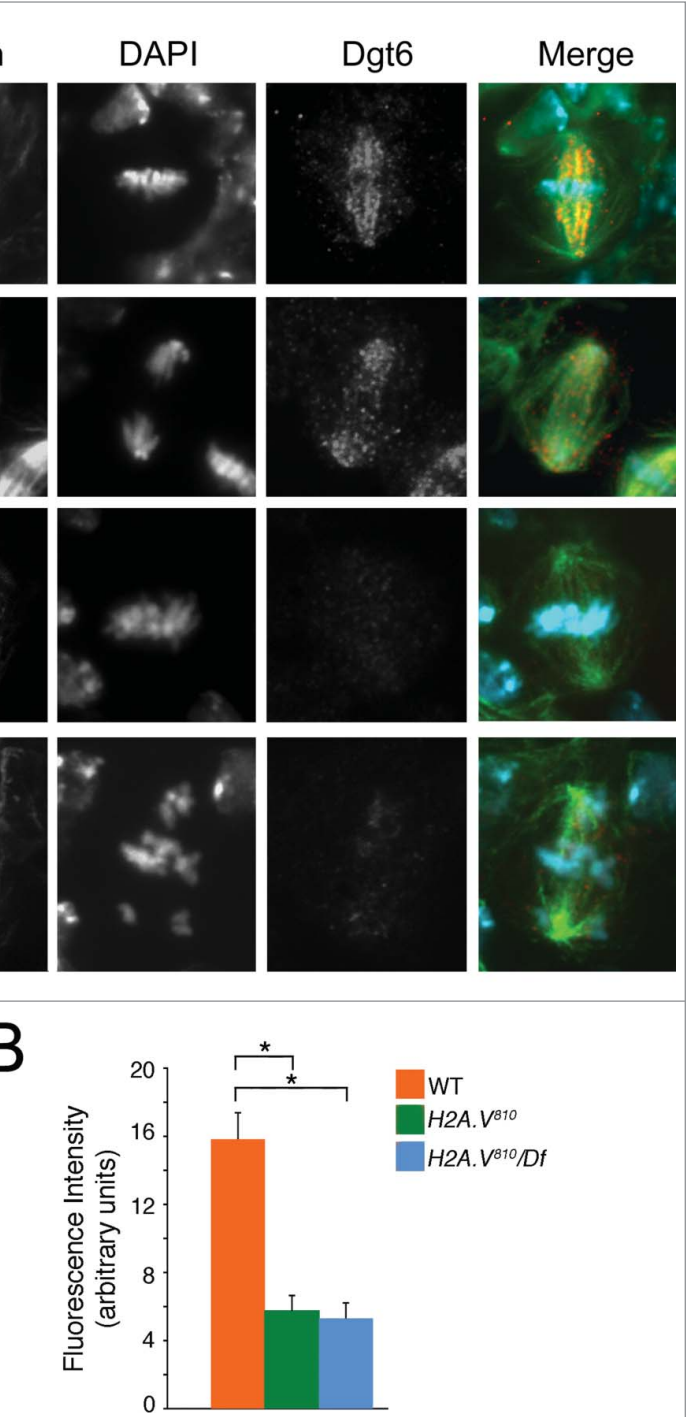
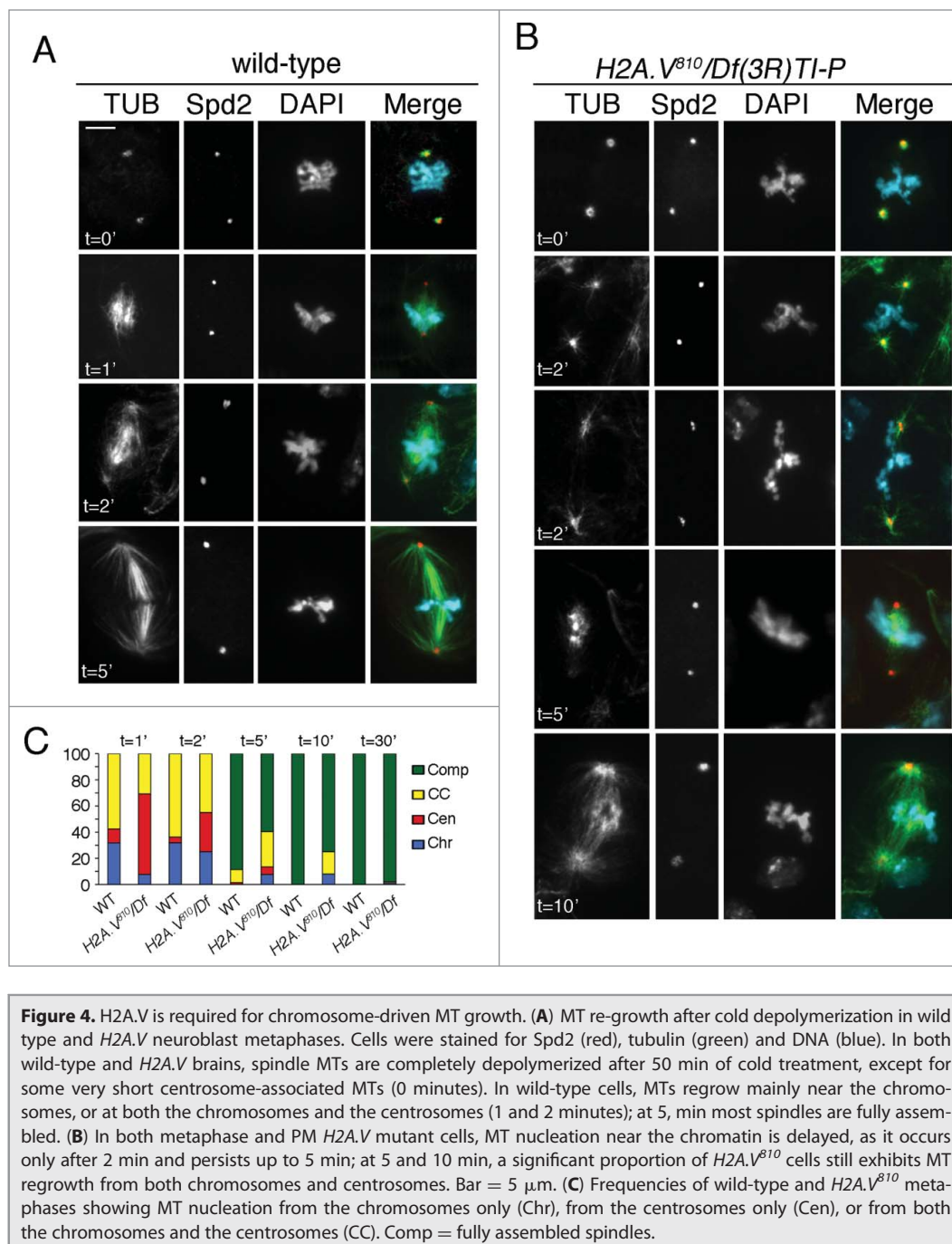


**Figure 3.** Dgt6 fails to localize at MTs of *H2A.V*<sup>B10</sup> mutant cells. (A) Localization of Dgt6 in a wild-type NB metaphase (Aa), wild-type anaphase (Ab), in *H2A.V* mutant metaphase (Ac) and PA (Ad). (B) Quantification of Dgt6 localization (bars indicate SEM; 50 cells analyzed for each genotype, \**P* < 0.01, *t* Student's Test).

directly or indirectly by the HP1 N-terminal domain (Fig. 6C).

#### Loss of HP1 impairs kinetochore-driven MT formation

Our analysis of the functional relationship between *H2A.V* and HP1 led us to speculate that HP1 may also be involved in the



chromosomes.<sup>36</sup> This would mask the analysis of a potential centromere/kinetochore dysfunction. To circumvent this problem, we looked for mitotic defects in a *UAS HP1 RNAi* line that behaved as a hypomorphic *HP1* mutant allele (see Materials and Methods). By crossing *UAS HP1 RNAi* to the *69B GAL4*-bearing flies, we drew *HP1* depletion specifically in brains and observed a ~60% reduction of *HP1* levels and a frequency of telomeric associations lower than that observed for *Su(var)205* null alleles (data not shown). The cytological characterization of DAPI-stained no-colchicine treated larval brains revealed that the MI and the AF in the *HP1 RNAi* neuroblasts are comparable to wild-type (data not shown). This indicates that, consistent with published data<sup>36,37</sup> and unlike *H2A.V<sup>810</sup>* mutants, cells without *HP1* are still able to complete mitosis. To determine whether cells lacking *HP1* demonstrated the PA phenotype observed in *H2A.V<sup>810</sup>* mutants, we analyzed a sample of cells with no telomeric fusions. Of these, 5% ( $n = 200$ ) had chromosomes scattered across the major axis of the cytoplasm, reminiscent of the PAs observed in *H2A.V<sup>810</sup>* mutants. It is also

organization of kinetochore-fibers. We thus asked whether loss of *HP1* could phenocopy the cell division defects seen in *H2A.V<sup>810</sup>* mutants. We performed a cytological characterization of mitosis in *Su(var)205/HP1* mutants and checked for the presence of PAs and/or metaphases with defects in kinetochore-driven MT formation. It is well known that null mutations in the *Su(var)205/HP1* gene cause frequent telomere fusions in *Drosophila* larval brain cells, leading to the formation of trains of chromosomes.<sup>36</sup> These multiple telomeric associations give rise to frequent chromosome bridges and segregation defects during anaphase leading to hyperploid and polyploid cells with either fused or broken

worth noting that this frequency may not be representative of the overall rate of PAs, because cells with telomeric fusions were excluded from the count because the fusion of chromosomes impedes the observation of PAs.

Anti- $\alpha$  tubulin and anti-Spd2 immunostainings revealed that ~75% ( $n = 140$ ) of dividing cells exhibited normal bipolar spindles, with the remaining cells displaying either multipolar (~8%) or monopolar (~17%) spindle. While multipolar spindles were associated with hyperploid/polyploid cells, the presence of few monopolar spindles suggests that loss of *HP1* might affect spindle assembly (Fig. S4A). This result is important in that it

demonstrates phenotypic similarities with *H2A.V<sup>810</sup>* PAs, which also exhibited normal bipolar spindles (Fig. 7A, C). It also lends support to the hypothesis that PAs do not arise from spindle alteration. We also found that *HP1* mutant PA chromosomes show a normal localization of centromeric antigens, a robust localization of the SAC protein BubR1 and high levels of cyclin B. This confirms that, like *H2A.V* mutant cells, these mutants never move into metaphase (Fig. S4B, C). Moreover, Dgt6 localization was significantly reduced in the majority of mutant dividing cells (Fig. 7A, B), suggesting that *HP1* depleted cells, alike *H2A.V<sup>810</sup>* mutant cells, may experience defects in kinetochore-driven MT formation.

To confirm these observations, we performed a MT regrowth assay after cold-treatment. We found that *HP1* depleted cells exhibit a scarce MT regrowth from chromosomes after 1 min recovery, with the majority of cells showing MT re-growth from centrosomes (Fig. 7E; see Fig. 4C for comparison). Even after 2 min recovery, MTs were found to re-grow mainly from centrosomes (~30%) and very few (~2%) from chromosomes (n = 40). Finally, after 5 min similarly to the *H2A.V<sup>810</sup>* mutants, only ~40% of *HP1* mutant cells (n = 35) completed spindle formation, whereas a full developed spindle is already seen in almost all control cells (Fig. 7C; see Fig. 4C for comparison). Thus, we can conclude that, in addition to protecting telomeres from fusion events and regulating gene expression, *HP1*, like *H2A.V*, is required for establishing a correct kinetochore-driven MT formation during mitosis.

Taken together, our data suggest that chromosome segregation defects seen upon depletion of *H2A.V* are mainly caused by the loss of *HP1* from centromeres. To test this hypothesis, we overexpressed *HP1* in *H2A.V<sup>810</sup>* mutants. We found that the expression of a [*RFP-HP1*] transgene yields a 2-fold increase of *HP1* levels (data not shown) and, when expressed in *H2A.V<sup>810</sup>* mutant background, is able to reduce the frequency of PAs from 20% to 5% (n = 130). This confirms our hypothesis that chromosome misalignments in *H2A.V<sup>810</sup>* mutant cells are mainly due to reduced *HP1* levels. MT re-growth analysis shows that 1 and 2 min after cold treatment, the proportion of the *HP1*-expressing *H2A.V<sup>810</sup>* mutant neuroblasts showing microtubule re-growth from kinetochore and from both kinetochore and centrosomes is

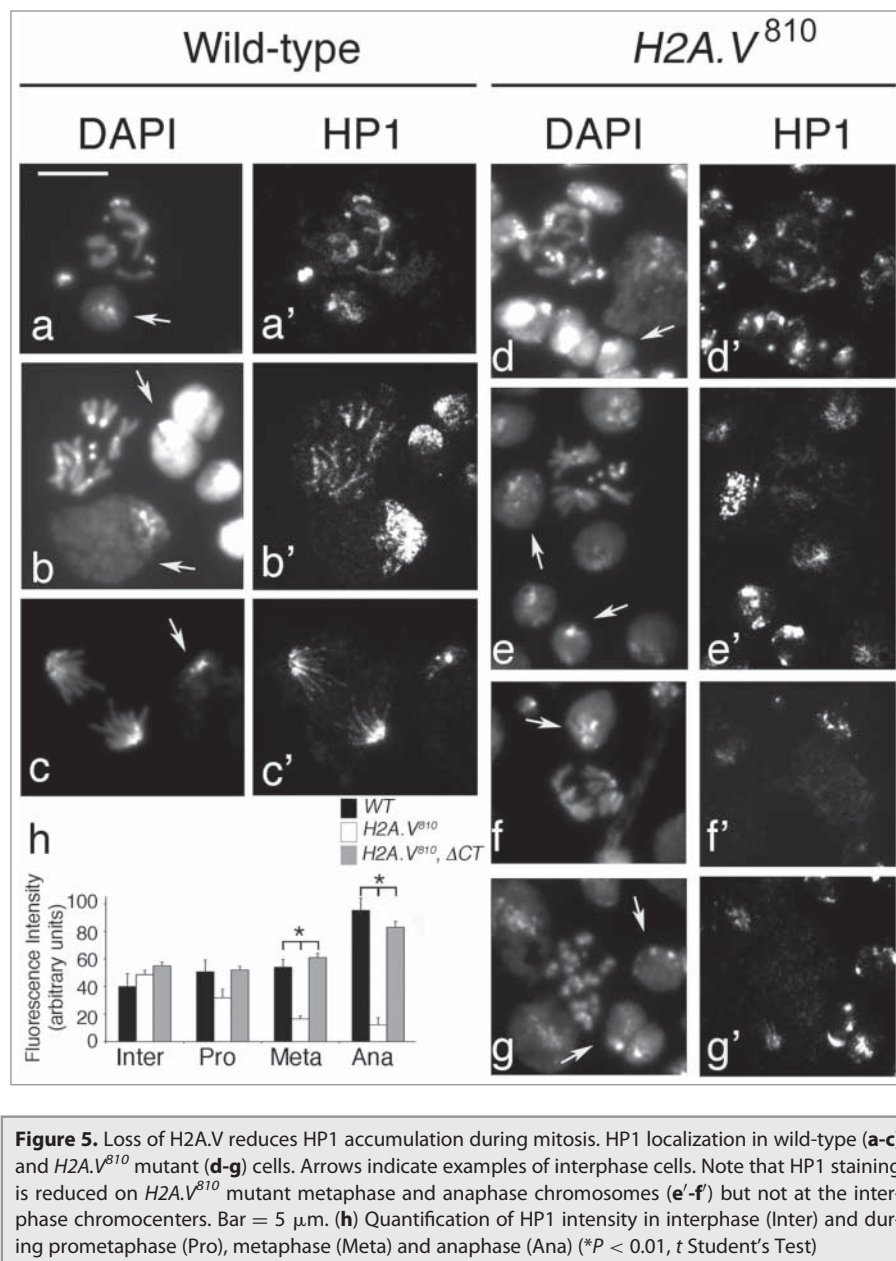


**Figure 5.** Loss of *H2A.V* reduces *HP1* accumulation during mitosis. *HP1* localization in wild-type (a-c) and *H2A.V<sup>810</sup>* mutant (d-g) cells. Arrows indicate examples of interphase cells. Note that *HP1* staining is reduced on *H2A.V<sup>810</sup>* mutant metaphase and anaphase chromosomes (e'-f') but not at the interphase chromocenters. Bar = 5  $\mu$ m. (h) Quantification of *HP1* intensity in interphase (Inter) and during prometaphase (Pro), metaphase (Meta) and anaphase (Ana) (\* $P < 0.01$ , *t* Student's Test)

higher than that seen in *H2A.V<sup>810</sup>* mutants and very similar to wild-type (Fig. 7C; see also Fig. 4C for comparison), indicating that *HP1* transgene rescues defects in the kinetochore-driven MT formation. As consequence after 5 min of recovery from cold, fully formed mitotic spindles are much more frequent in [*RFP-HP1*] *H2A.V<sup>810</sup>* recombinants (~80% of cells; n = 30) compared to *H2A.V<sup>810</sup>* mutants (Fig. 7C and Fig. 4C for a direct comparison) confirming that additional copies of *HP1* ameliorate spindle assembly when *H2A.V* is lost. However, a significant fraction of cells showing microtubule growth from centrosomes or kinetochores is still present in the [*RFP-HP1*] *H2A.V<sup>810</sup>* recombinant brains, so *HP1* overexpression alone is not sufficient to fully restore functional spindles. Thus, a simultaneous presence of *H2A.V* and *HP1* is required to fulfill a proper spindle behavior.



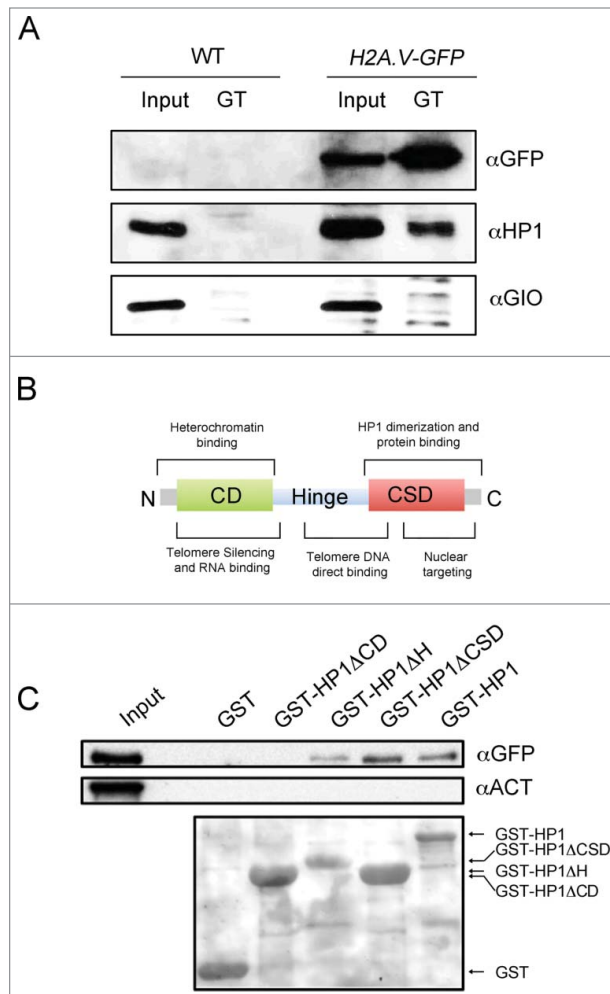


**Figure 6.** H2A.V interacts with HP1. **(A)** GFP-Trap immunoprecipitation (GT) from wild type and H2A.V-GFP expressing brain extracts. Giotto (GIO)<sup>55</sup> has been used as loading control. **(B)** The HP1 protein domains (adapted from Fanti and Pimpinelli (2008)<sup>35</sup>). **(C)** GST-pulldown of H2A.V-GFP expressing brain extracts with GST-tagged HP1 (GST-HP1) and HP1 truncations in which either the Chromo domain (GST-HP1 $\Delta$ CD), the Hinge (GST-HP1 $\Delta$ H) or the Chromo Shadow domain (GST-HP1 $\Delta$ CSD) has been deleted.

## Discussion

Here, we provide compelling evidence that H2A.V, the *Drosophila* histone H2A variant, plays an important and unanticipated role during *Drosophila* mitosis. The cytological characterization of *H2A.V*<sup>810</sup> mutant larval brain chromosomes revealed that loss of H2A.V has an impact on chromosome organization and cell proliferation (Fig. 1), which is consistent with previous results on a role of this histone variant in chromatin remodeling and heterochromatin organization.<sup>20,26,27</sup> We also demonstrate that a significant proportion of *H2A.V* mutant cells fails to complete mitosis and contains chromosomes that remain scattered across the spindle (pseudo anaphase or PA) due to failed metaphase plate alignment. Similar effects have been previously described in *Drosophila* S2 cells depleted by RNAi of either

kinetochore proteins, augmin components or splicing factors.<sup>29,30</sup> However unlike those S2 interfered cells, which exhibit PAs with long spindles, *H2A.V*<sup>810</sup> mutant cells have PA spindles that appear similar to wild type anaphases. The reason why *H2A.V* mutant cells are not elongated is unclear, but it may depend on the different cellular systems employed in the different studies. Intriguingly, the presence of PAs in *H2A.V*<sup>810</sup> mutants indicates for the first time that *Drosophila* H2A.V is also necessary for chromosome segregation.

Interestingly, our results from both Dgt6 immunolocalization and spindle microtubule re-growth assay following cold-induced MT depolymerization in mitotic neuroblasts reveal that H2A.V might be involved in the organization of kinetochore-driven k-fibers. However, we believe that defects in the organization of k-fibers are not a consequence of the reduction of Dgt6. Recent studies demonstrated that *Wac*, a newly discovered component of Augmin complex, is required for spindle formation in S2 cells but is dispensable for somatic mitosis. In fact, a *wac* deletion mutant was viable and displayed only weak defects in brain cell divisions, suggesting that the components of Augmin complex (including Dgt6) might have non essential roles in spindle assembly.<sup>38</sup>

It has been previously reported that defective k-fiber formation and elongation disrupt chromosome segregation and spindle formation in *Drosophila* cells.<sup>29</sup> Our results, which are in line with this finding, indicate that a specific chromatin organization is also necessary to ensure a proper spindle assembly. We speculate that the observed PAs are a result of improper organization of k-fibers, and that PAs fail to complete mitosis, thus reducing in part the frequency of anaphases in *H2A.V*<sup>810</sup> mutants. It is also plausible that persistent chromosome misalignment leads to a mitotic arrest of these cells, which in turn could explain the presence of *H2A.V*<sup>810</sup> mutant cells with overcondensed chromosomes (Fig. 1). However, while in Bucciarelli et al (2009) the presence of PAs was always associated to a strong increase of mitotic index (MI), in our mutants the MI did not change. One explanation is that the reduction of anaphase frequency in *H2A.V*<sup>810</sup> mutants (20%) is not as dramatic as that reported for Dgt6-depleted S2 cells (50%)<sup>29</sup> and therefore it unlikely affects mitotic progression. An alternative explanation is that loss of H2A.V might affect the regulation of G2-M and/or M-A cell cycle checkpoints thus preventing a metaphase arrest. Further investigations are required to verify this hypothesis. It is worth noting that, although a role for H2A.Z in chromosome segregation has been previously documented in human and yeast cells,<sup>12,13,39-42</sup> our data provide the first evidence of a potential involvement of H2A.Z in the organization of k-fibers.

We also provide unanticipated molecular evidence that H2A.V interacts directly or indirectly with HP1, confirming that both proteins are part of same complex (see also Ref 27). It is intriguing that the H2A.V-HP1 interaction depends on the HP1 CD domain, which also binds H3K9me2/3 and mediates heterochromatin formation.<sup>43</sup> This supports the existence of a cascade of events that requires the recruitment of H2A.V and different histone modifications for the establishment of heterochromatin.<sup>26</sup> Yet, the reason why depletion of H2A.V causes a direct loss of HP1 and particularly during mitosis is unclear. Nonetheless, as

HP1 overexpression in *H2A.V* mutant cells prevents PA formation, we speculate that a *H2A.V*-dependent stabilization/localization of HP1 at centromeric region is essential to ensure proper chromosomal behavior.

Previous studies have shown that *H2A.Z* alters the nucleosomal surface, thus enabling preferential binding of HP1a to condensed higher chromatin structures.<sup>44</sup> It is conceivable then that the *H2A.V*-HP1 interaction is favored by the condensation of pericentric chromatin fiber in metaphase. Alternatively, these interactions may be encouraged by metaphase-specific posttranslational modifications of *H2A.V*, HP1 or other interacting proteins. Indeed, it has been proposed the mechanism underpinning HP1 recruitment on mitotic chromosomes might be different from that in interphase.<sup>45</sup> Still, little is known about the factors required for specific localization of HP1 at mitotic centromeres save for a few discoveries. Human HP1 $\alpha$  binding to INCENP, for instance, has been demonstrated as necessary for HP1 $\alpha$  targeting to mitotic centromeres. We believe that *H2A.V* may play a similar role in mediating HP1 binding,<sup>46-48</sup> but how this takes place remains to be seen.

Our functional characterization of *H2A.V* has also unveiled the role of *Drosophila* HP1a in the assembly of the mitotic spindle. Our results indicate that the loss of HP1 yields defects in the kinetochore-driven k-fiber organization, which can in turn compromise chromosome segregation thus generating PAs. Past studies have shown that HP1a contributes to chromosome segregation and centromere stability in a variety of organisms including mammals,<sup>49,50</sup> but the mechanism is still not completely understood. HP1 is known to interact with components of the centromere and the kinetochore complex,<sup>47,51</sup> providing targets to begin understanding how downregulation or mislocalization of HP1 result in mitotic defects.<sup>51-53</sup> It has also been reported that in contrast to Swi6 in *S. pombe*, the correct localization of HP1 is not required for the recruitment of cohesins to centromeric regions in mammals.<sup>54</sup> Yet, HP1a seems to help in protecting cohesins from degradation by recruiting the Shugoshin protein.<sup>45</sup> Here, we have highlighted an additional function of HP1 during chromosome

segregation, one which depends on interaction with *H2A.V* and is required to regulate k-fiber organization. These results thus provide further evidence of a functional versatility of HP1 that is likely conserved also in mammals.

## Materials and Methods

### Drosophila strains

The *l(3)H2A.V<sup>810</sup>* mutant line, *Df(3R)TI-P* deficiency that uncovers *H2A.V*, the *P [RFP-HP1]* stock, and the *Su(var)205<sup>HMS00278</sup>* (*HP1 RNAi*) line were obtained from the Bloomington Stock Center. The *H2A.V-gfp* transgene was obtained from R. Saint and the C-terminally truncated (*H2A.V<sup>ACT</sup>*) rescue constructs from Y. Rong (NCI, NHI, Bethesda, MD). Both lines were previously described.<sup>9</sup> The *69B GAL4* driver, which expresses GAL4 in brains, was obtained from the Vienna Drosophila RNAi center (VDRC). The *[RFP-HP1] H2A.V<sup>810</sup>* bearing chromosome were obtained by recombination and balanced over *TM6c*. Information on the genetic markers and balancers used in this study is available at Flybase (<http://flybase.bio.indiana.edu/>). Stocks were maintained and crosses were made on standard *Drosophila* medium at 25°C.

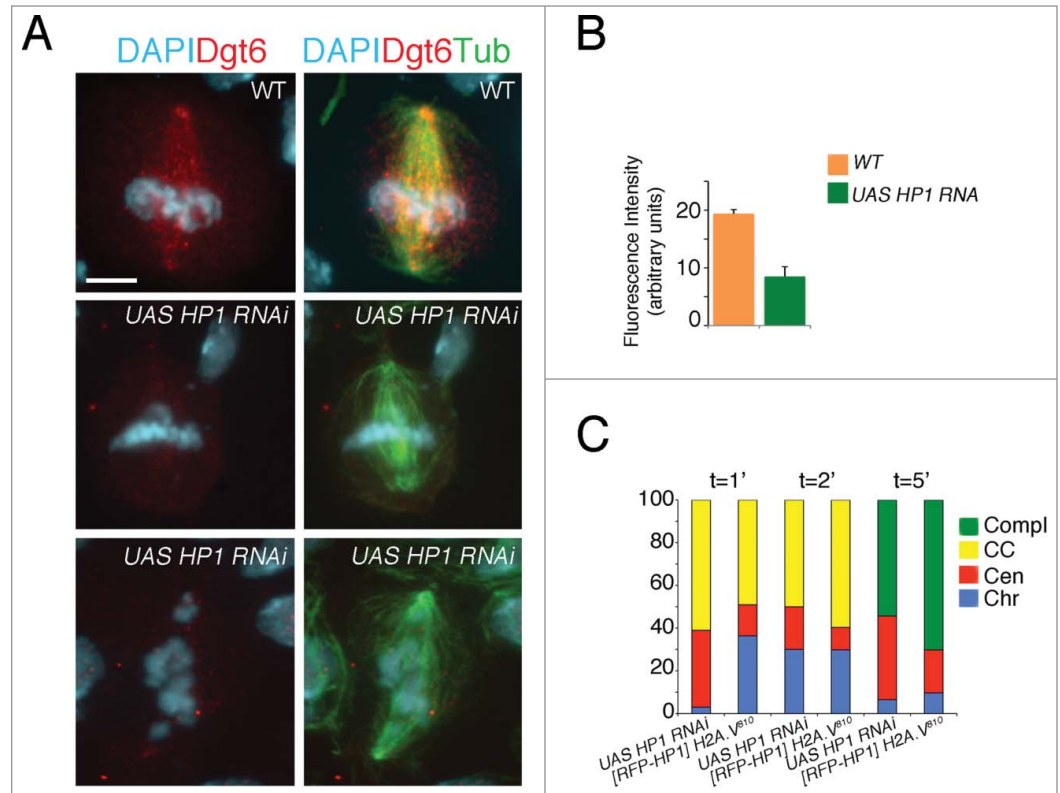


**Figure 7.** HP1 is required for cell division. (A) Dgt6 fails to localize at MTs of *HP1* mutant metaphases (central panel) and PAs (bottom). (B) Quantification of Dgt6 localization (bars indicate SEM). A total number of 50 (WT) and 100 (*HP1* mutant) cells were analyzed (C) Frequencies of *HP1* mutant cells and *H2A.V<sup>810</sup>* mutant cells expressing the *[RFP-HP1]* transgene showing MT regrowth after cold. Loss of HP1 delays MT regrowth from kinetochores as observed in *H2A.V<sup>810</sup>* mutants. Note that HP1 overexpression increases the number of *H2A.V<sup>810</sup>* mutant cells with MT nucleation form chromosomes (Chr) and from both chromosomes and centrosomes (CC; see Fig. 4 for comparison).

### Chromosome cytology and immunostaining

DAPI-stained brain squashes were obtained according to published methods.<sup>56</sup> Microtubule regrowth after cold was performed as previously described.<sup>34</sup> HP1 immunostaining of mitotic chromosomes was carried out according to Fanti et al. (1998).<sup>36</sup> Brain squashes for H2A.V immunostaining were prepared as previously indicated.<sup>57</sup> For the other immunostaining experiments, brains from third instar larvae were dissected and fixed as previously described.<sup>58</sup> After several rinses in phosphate buffered saline 0.1% Triton (PBS-T) brain preparations were incubated overnight at 4°C with primary antibodies diluted in PBS. After two rinses in PBS these primary antibodies were detected by incubation for 1 h with the appropriate secondary antibody. We used the following primary antibodies: anti- $\alpha$  tubulin monoclonal (1:1000, Sigma), rabbit anti-Spd2 (1:3500),<sup>28</sup> rabbit anti-ZW10 (1:100),<sup>32</sup> rabbit anti-cyclin B (1:2000) and rabbit anti-CENP-C (1:100) (gifts of Christian Lehner, Zurich, Switzerland), Chicken anti-CID (1:5000),<sup>59</sup> rabbit anti-BubR1 (1:500), rabbit anti-Mis12 (1:100) and rabbit anti Nsl-1(1:100) (gifts from David Glover University of Cambridge, England), and rabbit anti-Ncd80 (1:50) (gifts of M. Goldberg, Cornell University Ithaca NY) rabbit-anti-Dgt6 (1:100),<sup>29</sup> rabbit anti-H2AV (1:50; gift of V. Corces; Johns Hopkins University, Baltimore, MD), mouse monoclonal anti-HP1 (C1A9; 1:20, developed by L.Wallrath, University of Iowa, Iowa City, IA and obtained from the Developmental Studies Hybridoma Bank, created by the NICHD of the NIH and maintained at The University of Iowa, Department of Biology, Iowa City, IA). The secondary antibodies were FITC-conjugated anti-mouse (1:100), Cy3-conjugated anti-rabbit (1:300), or Cy3-conjugated anti-chicken IgGs (1:100), all from Jackson Laboratories. All preparations are mounted in Vectashield H-1200 with DAPI (Vector Laboratories) to stain the chromosomes and examined with a Zeiss Axioplan microscope, equipped with an HBO100W mercury lamp and a cooled charged-coupled device (CCD camera; Photometrics CoolSnap HQ). Grayscale images were collected separately, converted to Photoshop (Adobe Systems), pseudocolored and merged.

To estimate the MT density, the Dgt6 and the HP1 fluorescence in wild-type and mutant cells, we used the ImageJ software ([rsb.info.nih.gov/ij/](http://rsb.info.nih.gov/ij/)). Mean pixel intensities of fluorescence were measured within a fixed region and the fluorescence intensity of an area adjacent to the region of interest was used for background subtraction. In particular, to quantify MT fluorescence intensity we considered a spindle area near (but not including) the chromosomes and an identical spindle area near the poles. Dgt6 was quantified considering a spindle area near (but not including) the chromosomes. To measure HP1 fluorescence intensity, we considered an area including the chromocenter in interphase nuclei, and an area including the pericentromeric regions of prophase, metaphase and anaphase chromosomes.

### Production and purification of recombinant proteins

To obtain GST-HP1, -HP1<sup>ACD</sup>, -HP1<sup>ΔH</sup> and -HP1<sup>ACSD</sup> fusion proteins, the corresponding cDNAs were cloned in the pGEX-6P1 vectors as described previously.<sup>60</sup> Bacterially

expressed GST fusion proteins were purified by incubating crude lysates with glutathione sepharose beads (QIAGEN) as recommended by the manufacturer.

### Protein extract preparation, GST pulldown and Western Blot

To obtain extracts for GST-pulldown, GFP-Trap and Western Blot analysis, dissected third instar larval brains were lysed in an ice-cold buffer containing 20 mM Hepes KOH pH 7.9, 1.5 mM MgCl<sub>2</sub>, 10 mM KCl, 420 mM NaCl, 30 mM NaF, 0.2 mM Na<sub>3</sub>VO<sub>4</sub>, 25 mM BGP, 0.5 M PMSE, 0.1% NP40, 1c protease inhibitor cocktail (Roche).

For GST-pulldown and GFP-trap assays, protein extracts from ~50 brains were incubated with 2 μg of each GST fusion protein bound to sepharose beads in a buffer containing 20 mM Hepes KOH, 20 mM NaF and 0.8% NP40 for 1 h at 4°C. Sepharose-bound GST proteins were collected by centrifugation and washed several times with 20 mM Hepes KOH, 20 mM NaF and 1.8% NP40.

For immunoblotting, protein samples were resuspended in 1X Laemmli Buffer, run into SDS polyacrylamide gels and electroblotted on a nitrocellulose membrane (Bio-Rad) in a phosphate buffer containing 390 mM NaH<sub>2</sub>PO<sub>4</sub>H<sub>2</sub>O and 610 mM Na<sub>2</sub>HPO<sub>4</sub>H<sub>2</sub>O. After blocking with 5% low-fat dry milk, the membrane was probed with appropriate primary antibody. The blots were developed by the ECL or ECL Plus method (Amersham Biosciences) and signals detected with the ChemiDoc scanning system (BioRad). We used the following primary antibodies: monoclonal mouse anti-HP1 (C1A9; 1:500), rabbit anti-GFP (1:1000; a gift from G. Cestra, CNR, Rome, IT), anti-actin HRP conjugated (1:10000; Roche). Secondary antibodies were: sheep anti-mouse IgG HRP-conjugated (1:5000), or donkey anti-rabbit IgG HRP-conjugated (1:5000) (both from Amersham Biosciences).

Quantification of band intensities was obtained by using the densitometry software ImageJ.

### Disclosure of Potential Conflicts of Interest

No potential conflicts of interest were disclosed.

### Acknowledgments

We thank V. Corces, ML. Goldberg, G. Cestra, Y. Rong, C. Lehner, D. Glover and M. Gatti for providing reagents. We thank M.Gatti, P. Somma, J. Blum and members of Cenci lab for critical reading of the manuscript.

### Funding

This work was funded by grants of Italian Association for Cancer Research (AIRC, IG 12749) to G.C and Progetto di Ateneo (Sapienza University of Rome) to F.V and G.C.

### Supplemental Material

Supplemental data for this article can be accessed on the publisher's website.

## References

1. Kornberg RD, Thomas JO. Chromatin structure; oligomers of the histones. *Science* 1974; 184:865-8; PMID:4825888; <http://dx.doi.org/10.1126/science.184.4139.865>
2. Luger K, Mader AW, Richmond RK, Sargent DF, Richmond TJ. Crystal structure of the nucleosome core particle at 2.8 Å resolution. *Nature* 1997; 389:251-60; PMID:9305837; <http://dx.doi.org/10.1038/38444>
3. Bannister AJ, Kouzarides T. Regulation of chromatin by histone modifications. *Cell Res* 2011; 21:381-95; PMID:21321607; <http://dx.doi.org/10.1038/cr.2011.22>
4. Kouzarides T. Chromatin modifications and their function. *Cell* 2007; 128:693-705; PMID:17320507; <http://dx.doi.org/10.1016/j.cell.2007.02.005>
5. Ruthenburg AJ, Li H, Patel DJ, Allis CD. Multivalent engagement of chromatin modifications by linked binding modules. *Nat Rev Mol Cell Biol* 2007; 8:983-94; PMID:18037899; <http://dx.doi.org/10.1038/nrm2298>
6. Henikoff S, Ahmad K. Assembly of variant histones into chromatin. *Ann Rev Cell Dev Biol* 2005; 21:133-53; PMID:16212490; <http://dx.doi.org/10.1146/annurev.cellbio.21.012704.133518>
7. Malik HS, Henikoff S. Phylogenomics of the nucleosome. *Nat Struct Biol* 2003; 10:882-91; PMID:14583738; <http://dx.doi.org/10.1038/nsb996>
8. Liu X, Li B, Gorovsky MA. Essential and nonessential histone H2A variants in *Tetrahymena thermophila*. *Mol Cell Biol* 1996; 16:4305-11; PMID:8754831
9. Clarkson MJ, Wells JR, Gibson F, Saint R, Tremethick DJ. Regions of variant histone H2Av required for *Drosophila* development. *Nature* 1999; 399:694-7; PMID:10385122; <http://dx.doi.org/10.1038/21436>
10. Ridgway P, Brown KD, Rangasamy D, Svensson U, Tremethick DJ. Unique residues on the H2A.Z containing nucleosome surface are important for *Xenopus laevis* development. *J Biol Chem* 2004; 279:43815-20; PMID:15299007; <http://dx.doi.org/10.1074/jbc.M408409200>
11. Faast R, Thonglairoam V, Schulz TC, Beall J, Wells JR, Taylor H, Matthaeci K, Rathjen PD, Tremethick DJ, Lyons L. Histone variant H2A.Z is required for early mammalian development. *Curr Biol* 2001; 11:1183-7; PMID:11516949; [http://dx.doi.org/10.1016/S0960-9822\(01\)00329-3](http://dx.doi.org/10.1016/S0960-9822(01)00329-3)
12. Ahmed S, Dul B, Qiu X, Walworth NC. Msc1 acts through histone H2A.Z to promote chromosome stability in *Schizosaccharomyces pombe*. *Genetics* 2007; 177:1487-97; PMID:17947424; <http://dx.doi.org/10.1534/genetics.107.078691>
13. Rangasamy D, Greaves I, Tremethick DJ. RNA interference demonstrates a novel role for H2A.Z in chromosome segregation. *Nat Struct Mol Biol* 2004; 11:650-5; PMID:15195148; <http://dx.doi.org/10.1038/nsmb786>
14. Hou H, Wang Y, Kallgren SP, Thompson J, Yates JR, 3rd, Jia S. Histone variant H2A.Z regulates centromere silencing and chromosome segregation in fission yeast. *J Biol Chem* 2010; 285:1909-18; PMID:19910462; <http://dx.doi.org/10.1074/jbc.M109.058487>
15. Draker R, Cheung P. Transcriptional and epigenetic functions of histone variant H2A.Z. *Biochem Cell Biol* 2009; 87:19-25; PMID:19234520; <http://dx.doi.org/10.1139/O08-117>
16. Guillemette B, Gaudreau L. Reuniting the contrasting functions of H2A.Z. *Biochem Cell Biol* 2006; 84:528-35; PMID:16936825; <http://dx.doi.org/10.1139/o06-077>
17. Greaves IK, Rangasamy D, Devoy M, Marshall Graves JA, Tremethick DJ. The X and Y chromosomes assemble into H2A.Z-containing [corrected] facultative heterochromatin [corrected] following meiosis. *Mol Cell Biol* 2006; 26:5394-405
18. Meneghini MD, Wu M, Madhani HD. Conserved histone variant H2A.Z protects euchromatin from the ectopic spread of silent heterochromatin. *Cell* 2003; 112:725-36; PMID:12628191; [http://dx.doi.org/10.1016/S0092-8674\(03\)00123-5](http://dx.doi.org/10.1016/S0092-8674(03)00123-5)
19. Sarcinella E, Zuzarte PC, Lau PN, Draker R, Cheung P. Monoubiquitylation of H2A.Z distinguishes its association with euchromatin or facultative heterochromatin. *Mol Cell Biol* 2007; 27:6457-68; PMID:17636032; <http://dx.doi.org/10.1128/MCB.00241-07>
20. Baldi S, Becker PB. The variant histone H2A.V of *Drosophila*—three roles, two guises. *Chromosoma* 2013; 122:245-58; PMID:23553272; <http://dx.doi.org/10.1007/s00412-013-0409-x>
21. Joyce EF, Pedersen M, Tiong S, White-Brown SK, Paul A, Campbell SD, McKim KS. *Drosophila* ATM and ATR have distinct activities in the regulation of meiotic DNA damage and repair. *J Cell Biol* 2011; 195:359-67; PMID:22024169; <http://dx.doi.org/10.1083/jcb.201104121>
22. Madigan JP, Chotkowski HL, Glaser RL. DNA double-strand break-induced phosphorylation of *Drosophila* histone variant H2Av helps prevent radiation-induced apoptosis. *Nucleic Acids Res* 2002; 30:3698-705; PMID:12202754; <http://dx.doi.org/10.1093/nar/gkf496>
23. van Daal A, Elgin SC. A histone variant, H2AvD, is essential in *Drosophila melanogaster*. *Mol Biol Cell* 1992; 3:593-602; PMID:1498368; <http://dx.doi.org/10.1091/mbc.3.6.593>
24. Hardy S, Jacques PE, Gevry N, Forest A, Fortin ME, Laflamme L, Gaudreau L, Robert F. The euchromatic and heterochromatic landscapes are shaped by antagonizing effects of transcription on H2A.Z deposition. *PLoS Genet* 2009; 5:e1000687; PMID:19834540; <http://dx.doi.org/10.1371/journal.pgen.1000687>
25. Leach TJ, Mazzeo M, Chotkowski HL, Madigan JP, Wotring MG, Glaser RL. Histone H2A.Z is widely but nonrandomly distributed in chromosomes of *Drosophila melanogaster*. *J Biol Chem* 2000; 275:23267-72; PMID:10801889; <http://dx.doi.org/10.1074/jbc.M910206199>
26. Swaminathan J, Baxter EM, Corces VG. The role of histone H2Av variant replacement and histone H4 acetylation in the establishment of *Drosophila* heterochromatin. *Genes Dev* 2005; 19:65-76; PMID:15630020; <http://dx.doi.org/10.1101/gad.1259105>
27. Messina G, Damia E, Fanti L, Atterrato MT, Celauro E, Mariotti FR, Accardo MC, Walther M, Verni F, Piccioni D, et al. Yeti, an essential *Drosophila melanogaster* gene, encodes a protein required for chromatin organization. *J Cell Sci* 2014; 127:2577-88; PMID:24652835; <http://dx.doi.org/10.1242/jcs.150243>
28. Giansanti MG, Bucciarelli E, Bonaccorsi S, Gatti M. *Drosophila* SPD-2 is an essential centriole component required for PCM recruitment and astral-microtubule nucleation. *Curr Biol* 2008; 18:303-9; PMID:18291647; <http://dx.doi.org/10.1016/j.cub.2008.01.058>
29. Bucciarelli E, Pellacani C, Naim V, Palena A, Gatti M, Somma MP. *Drosophila* Dgt6 interacts with Ndc80, Msps/XMAP215, and gamma-tubulin to promote kinetochore-driven MT formation. *Curr Biol* 2009; 19:1839-45; PMID:19836241; <http://dx.doi.org/10.1016/j.cub.2009.09.043>
30. Somma MP, Fasulo B, Cenci G, Cundari E, Gatti M. Molecular dissection of cytokinesis by RNA interference in *Drosophila* cultured cells. *Mol Cell Biol* 2002; 22:2448-60; PMID:12134082; <http://dx.doi.org/10.1091/mbc.01-12-0589>
31. Kares R. Rod-Zw10-Zwilch: a key player in the spindle checkpoint. *Trends Cell Biol* 2005; 15:386-92; PMID:15922598; <http://dx.doi.org/10.1016/j.tcb.2005.05.003>
32. Williams BC, Karr TL, Montgomery JM, Goldberg ML. The *Drosophila* l(1)zw10 gene product, required for accurate mitotic chromosome segregation, is redistributed at anaphase onset. *J Cell Biol* 1992; 118:759-73; PMID:1339459; <http://dx.doi.org/10.1083/jcb.118.4.759>
33. Goshima G, Mayer M, Zhang N, Stuurman N, Vale RD. Augmin: a protein complex required for centrosome-independent microtubule generation within the spindle. *J Cell Biol* 2008; 181:421-9; PMID:18443220; <http://dx.doi.org/10.1083/jcb.200711053>
34. Mottier-Pavie V, Cenci G, Verni F, Gatti M, Bonaccorsi S. Phenotypic analysis of misato function reveals roles of noncentrosomal microtubules in *Drosophila* spindle formation. *J Cell Sci* 2011; 124:706-17; PMID:21285248; <http://dx.doi.org/10.1242/jcs.072348>
35. Fanti L, Pimpinelli S. HP1: a functionally multifaceted protein. *Curr Opin Genet Dev* 2008; 18:169-74; PMID:18329871; <http://dx.doi.org/10.1016/j.gde.2008.01.009>
36. Fanti L, Giovinazzo G, Berloco M, Pimpinelli S. The heterochromatin protein 1 prevents telomere fusions in *Drosophila*. *Mol Cell* 1998; 2:527-38; PMID:9844626; [http://dx.doi.org/10.1016/S1097-2765\(00\)80152-5](http://dx.doi.org/10.1016/S1097-2765(00)80152-5)
37. Musaro M, Ciapponi L, Fasulo B, Gatti M, Cenci G. Unprotected *Drosophila melanogaster* telomeres activate the spindle assembly checkpoint. *Nat Genet* 2008; 40:362-6; PMID:18246067; <http://dx.doi.org/10.1038/ng.2007.64>
38. Meireles AM, Fisher KH, Colombie N, Wakefield JG, Ohkura H. Wac: a new Augmin subunit required for chromosome alignment but not for acentrosomal microtubule assembly in female meiosis. *J Cell Biol* 2009; 184:777-84; PMID:19289792; <http://dx.doi.org/10.1083/jcb.200811102>
39. Carr AM, Dorrington SM, Hindley J, Phear GA, Aves SJ, Nurse P. Analysis of a histone H2A variant from fission yeast: evidence for a role in chromosome stability. *Mol Gen Genet* 1994; 245:628-35; PMID:NOT\_FOUND; <http://dx.doi.org/10.1007/BF00282226>
40. Kim HS, Vanoosthuysen V, Fillingham J, Roguev A, Watt S, Kislinger T, Treyer A, Carpenter LR, Bennett CS, Emili A, et al. An acetylated form of histone H2A.Z regulates chromosome architecture in *Schizosaccharomyces pombe*. *Nat Struct Mol Biol* 2009; 16:1286-93; PMID:19915592; <http://dx.doi.org/10.1038/nsmb.1688>
41. Rangasamy D, Berven L, Ridgway P, Tremethick DJ. Pericentric heterochromatin becomes enriched with H2A.Z during early mammalian development. *EMBO J* 2003; 22:1599-607; PMID:12660166; <http://dx.doi.org/10.1093/emboj/cdgl60>
42. Sharma U, Stefanova D, Holmes SG. Histone variant H2A.Z functions in sister chromatid cohesion in *Saccharomyces cerevisiae*. *Mol Cell Biol* 2013; 33:3473-81; PMID:23816883; <http://dx.doi.org/10.1128/MCB.00162-12>
43. Jacobs SA, Taverna SD, Zhang Y, Briggs SD, Li J, Eisenberg JC, Allis CD, Khorasanizadeh S. Specificity of the HP1 chromo domain for the methylated N-terminus of histone H3. *EMBO J* 2001; 20:5232-41; PMID:11566886; <http://dx.doi.org/10.1093/emboj/20.18.5232>
44. Fan JY, Rangasamy D, Luger K, Tremethick DJ. H2A.Z alters the nucleosome surface to promote HP1alpha-mediated chromatin fiber folding. *Mol Cell* 2004; 16:655-61; PMID:15546624; <http://dx.doi.org/10.1016/j.molcel.2004.10.023>
45. Yamagishi Y, Sakuno T, Shimura M, Watanabe Y. Heterochromatin links to centromere protection by recruiting shugoshin. *Nature* 2008; 455:251-5; PMID:18716626; <http://dx.doi.org/10.1038/nature07217>
46. Kang J, Chaudhary J, Dong H, Kim S, Brautigam CA, Yu HT. Mitotic centromeric targeting of HP1 and its binding to Sgo1 are dispensable for sister-chromatid cohesion in human cells. *Mol Biol Cell* 2011; 22:1181-90; PMID:21346195; <http://dx.doi.org/10.1091/mbc.E11-01-0009>
47. Ainsztein AM, Kandels-Lewis SE, Mackay AM, Earnshaw WC. INCENP centromere and spindle targeting:

- Identification of essential conserved motifs and involvement of heterochromatin protein HP1. *J Cell Biol* 1998; 143:1763-74; PMID:9864353; <http://dx.doi.org/10.1083/jcb.143.7.1763>
48. Nozawa RS, Nagao K, Masuda HT, Iwasaki O, Hirota T, Nozaki N, Kimura H, Obuse C. Human POGZ modulates dissociation of HP1 alpha from mitotic chromosome arms through Aurora B activation. *Nat Cell Biol* 2010; 12:719-U212; PMID:20562864; <http://dx.doi.org/10.1038/ncb2075>
  49. Canzio D, Larson A, Narlikar GJ. Mechanisms of functional promiscuity by HP1 proteins. *Trends Cell Biol* 2014; 24:377-86; PMID:24618358; <http://dx.doi.org/10.1016/j.tcb.2014.01.002>
  50. Eissenberg JC, Elgin SC. HP1a: a structural chromosomal protein regulating transcription. *Trends Genet* 2014; 30:103-10; PMID:24555990; <http://dx.doi.org/10.1016/j.tig.2014.01.002>
  51. Obuse C, Iwasaki O, Kiyomitsu T, Goshima G, Toyoda Y, Yanagida M. A conserved Mis12 centromere complex is linked to heterochromatic HP1 and outer kinetochore protein Zwint-1. *Nat Cell Biol* 2004; 6:1135-U37; PMID:15502821; <http://dx.doi.org/10.1038/ncb1187>
  52. Auth T, Kunkel E, Grummt F. Interaction between HP1alpha and replication proteins in mammalian cells. *Exp Cell Res* 2006; 312:3349-59; PMID:16950245; <http://dx.doi.org/10.1016/j.yexcr.2006.07.014>
  53. Guenatri M, Bailly D, Maison C, Almouzni G. Mouse centric and pericentric satellite repeats form distinct functional heterochromatin. *J Cell Biol* 2004; 166:493-505; PMID:15302854; <http://dx.doi.org/10.1083/jcb.200403109>
  54. Koch B, Kueng S, Ruckenbauer C, Wendt KS, Peters JM. The Suv39h-HP1 histone methylation pathway is dispensable for enrichment and protection of cohesin at centromeres in mammalian cells. *Chromosoma* 2008; 117:199-210; PMID:18075750; <http://dx.doi.org/10.1007/s00412-007-0139-z>
  55. Giansanti MG, Bonaccorsi S, Kurek R, Farkas RM, Dimitri P, Fuller MT, Gatti M. The class I P1TP giotto is required for Drosophila cytokinesis. *Curr Biol* 2006; 16:195-201; PMID:16431372; <http://dx.doi.org/10.1016/j.cub.2005.12.011>
  56. Cenci G, Rawson RB, Belloni G, Castrillon DH, Tudor M, Petrucci R, Goldberg ML, Wasserman SA, Gatti M. UbcD1, a Drosophila ubiquitin-conjugating enzyme required for proper telomere behavior. *Genes Dev* 1997; 11:863-75; PMID:9106658; <http://dx.doi.org/10.1101/gad.11.7.863>
  57. Ciapponi L, Cenci G, Gatti M. The Drosophila Nbs protein functions in multiple pathways for the maintenance of genome stability. *Genetics* 2006; 173:1447-54; PMID:16648644; <http://dx.doi.org/10.1534/genetics.106.058081>
  58. Bonaccorsi S, Giansanti MG, Gatti M. Spindle assembly in Drosophila neuroblasts and ganglion mother cells. *Nat Cell Biol* 2000; 2:54-6; PMID:10620808; <http://dx.doi.org/10.1038/71378>
  59. Blower MD, Karpén GH. The role of Drosophila CID in kinetochore formation, cell-cycle progression and heterochromatin interactions. *N Cell Biol* 2001; 3:730-9; PMID:11483958; <http://dx.doi.org/10.1038/35087045>
  60. Raffa GD, Siriaco G, Cugusi S, Ciapponi L, Cenci G, Wojcik E, Gatti M. The Drosophila modigliani (moi) gene encodes a HOAP-interacting protein required for telomere protection. *Proc Natl Acad Sci U S A* 2009; 106:2271-6; PMID:19181850; <http://dx.doi.org/10.1073/pnas.0812702106>